Supplementary Information for

3D photothermal AFM-IR tomography at the nanometer scale

Alexandre Dazzi *et al.*

This PDF file includes:

Figs. S1 to S7

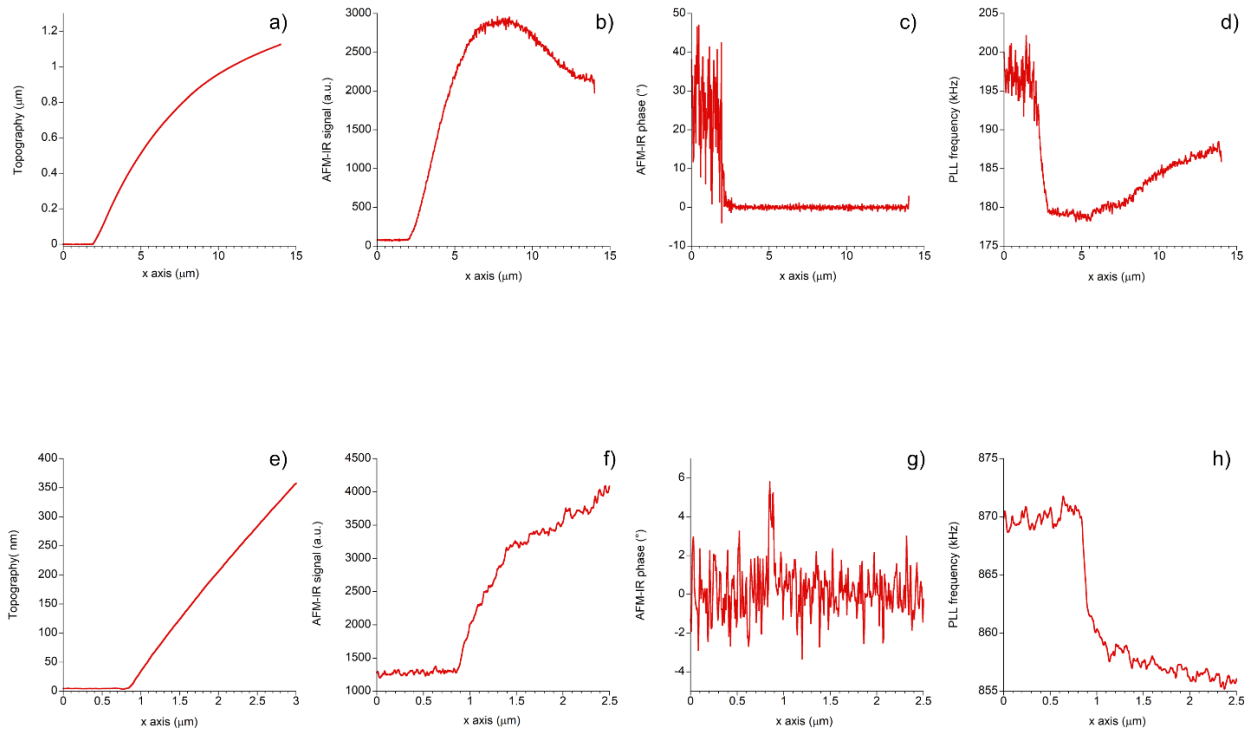

Fig. S1 : AFM-IR analysis comparing calibration wedges on different substrates. a) Topography line profile of the PMMA wedge on silicon substrate. b) Corresponding AFM-IR signal of the PMMA wedge absorption at 1730 cm^{-1}. The signal shows a maximum of absorption at the x position around 7 µm and a decrease thereafter. c) The AFM-IR phase shows a phase jump of about 30° even with activated PLL. d) The PLL frequency represents the variation of the laser frequency to match the resonance of the contact mode. e) Topography line profile of the PS wedge on PMMA substrate for comparison. f) Corresponding AFM-IR signal of the PS wedge absorption at 1600 cm^{-1}. The signal shows a continuous increase with the thickness as expected. g) The corresponding AFM-IR phase stays around zero demonstrating that the PLL works fine. A jump of 10° phase close to the x position at 0.8 µm is clearly associated with the beginning of the wedge. This jump is probably due to the change of lateral friction when the tip travels from PMMA to PS. h) The PLL follows the change of resonance even for a large range of frequencies from 870 kHz for PMMA to 855 kHz for PS.

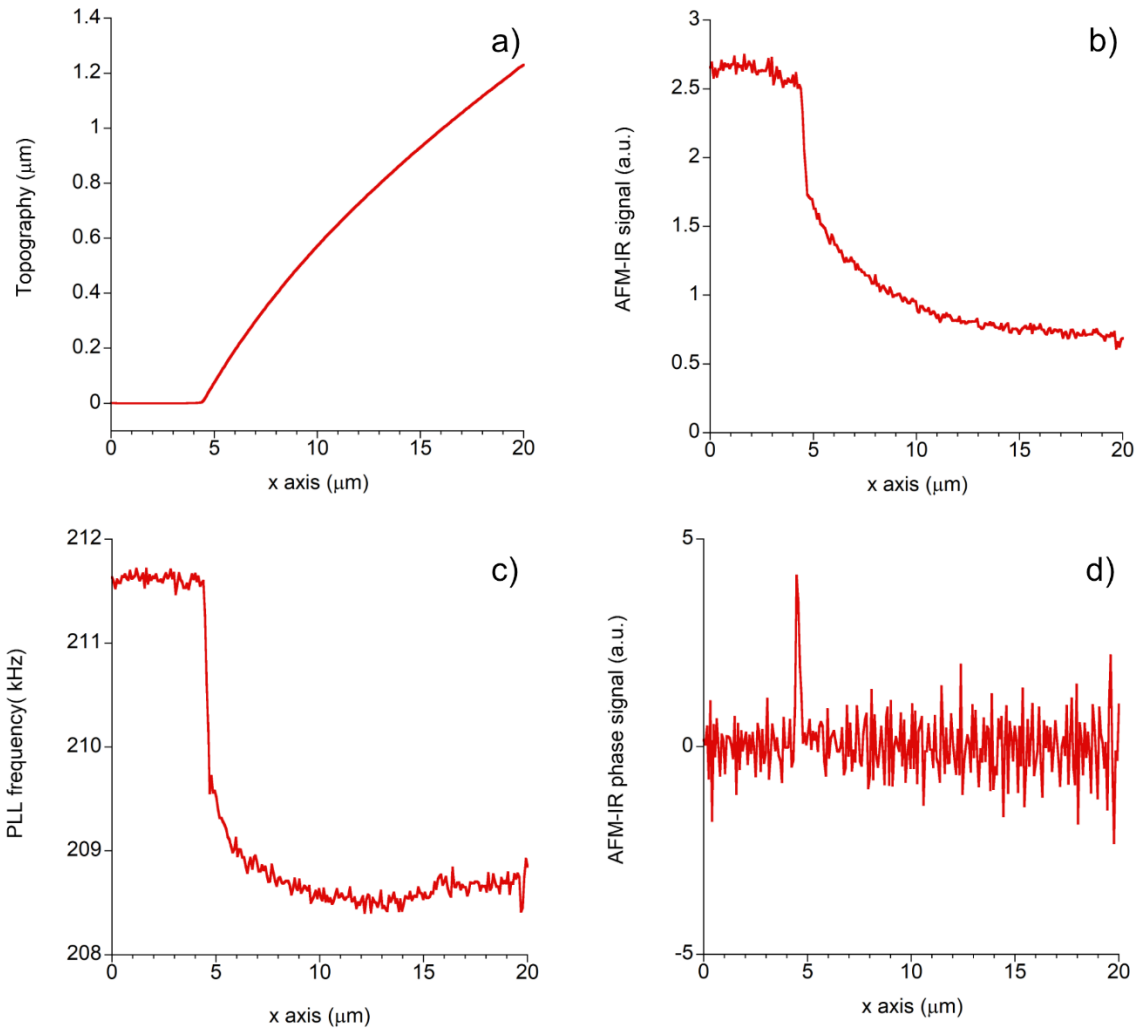

Fig. S2 : **AFM-IR analysis of PS wedge on PMMA matrix**. a) Topography line profile of the PS wedge on PMMA substrate. b) Corresponding AFM-IR signal of the PMMA substrate absorption at 1730 cm^{-1}. c) PLL frequency shows the variation of the contact resonance between the PMMA domain (211.5 kHz) and the PS domain (208.5 kHz). d) The AFM-IR phase is close to zero demonstrating that the PLL works correctly. A jump of 5° is present exactly at the beginning of the wedge probably translating a quick lateral friction change during the scan because of the transition from PMMA to PS.

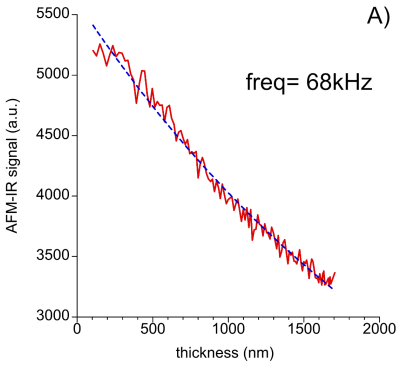

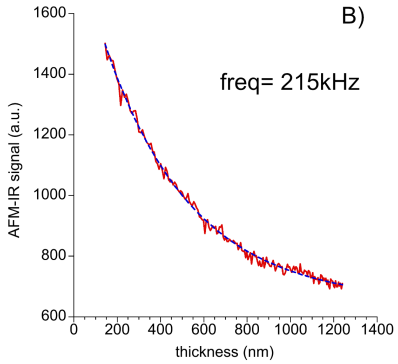

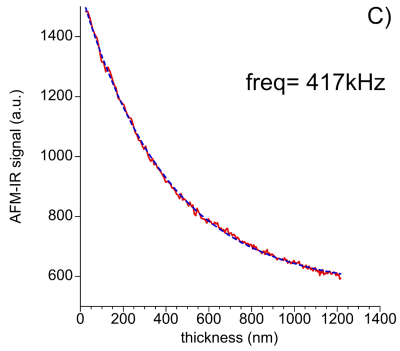

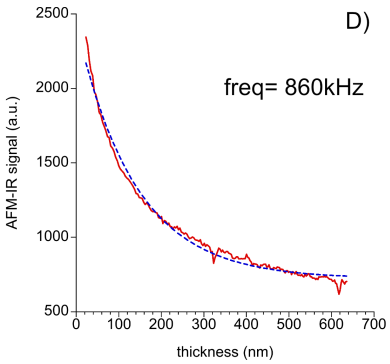

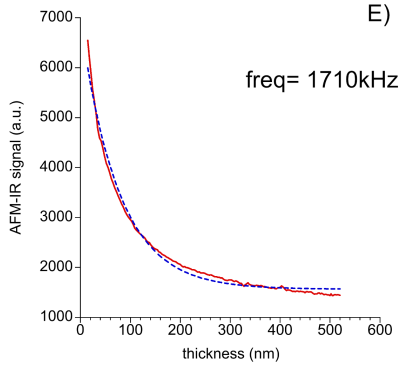

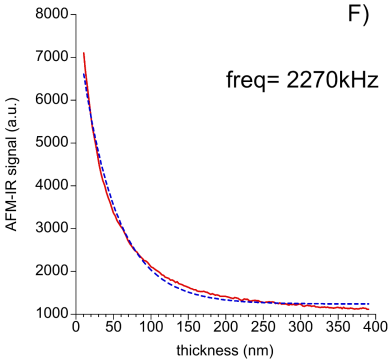

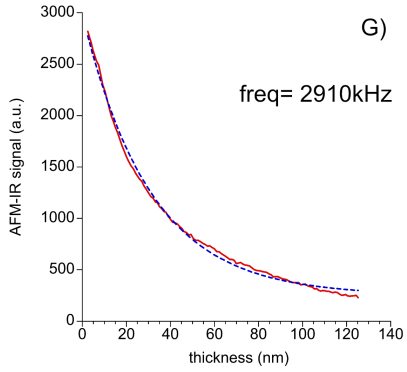

Table of fitting values for each mode

y=m1+m2*exp(-x/m3)

Mode	68 kHz	215 kHz	417 kHz	860 kHz	1710 kHz	2270 kHz	2910kHz
m1	212	650	559	731	1590	1257	251
m2	5360	1219	995	1706	5781	7136	2733
m3 (nm)	960	605	402	185	70	44	31
R	0.991	0.997	0.999	0.993	0.993	0.995	0.0998

Fig. S3 : Calibration of probing depth for HQ Mikromasch cantilever on the PS wedge on PMMA substrate for complementary resonance modes. The red curve corresponds to the contact AFM-IR signal as a function of the wedge thickness when the wave-number is fixed at 1730 cm-1 (PMMA absorption only). In dashed blue the corresponding fit is given of the exponential decay used to estimate the probing depth (m3) for respectively the following frequencies: A) 68 kHz, B) 215 kHz, C) 417 kHz, D) 860 kHz, E) 1710 kHz, F) 2270 kHz, G) 2910 kHz. The Table of fitting values represents all the fitting parameters for each corresponding mode.

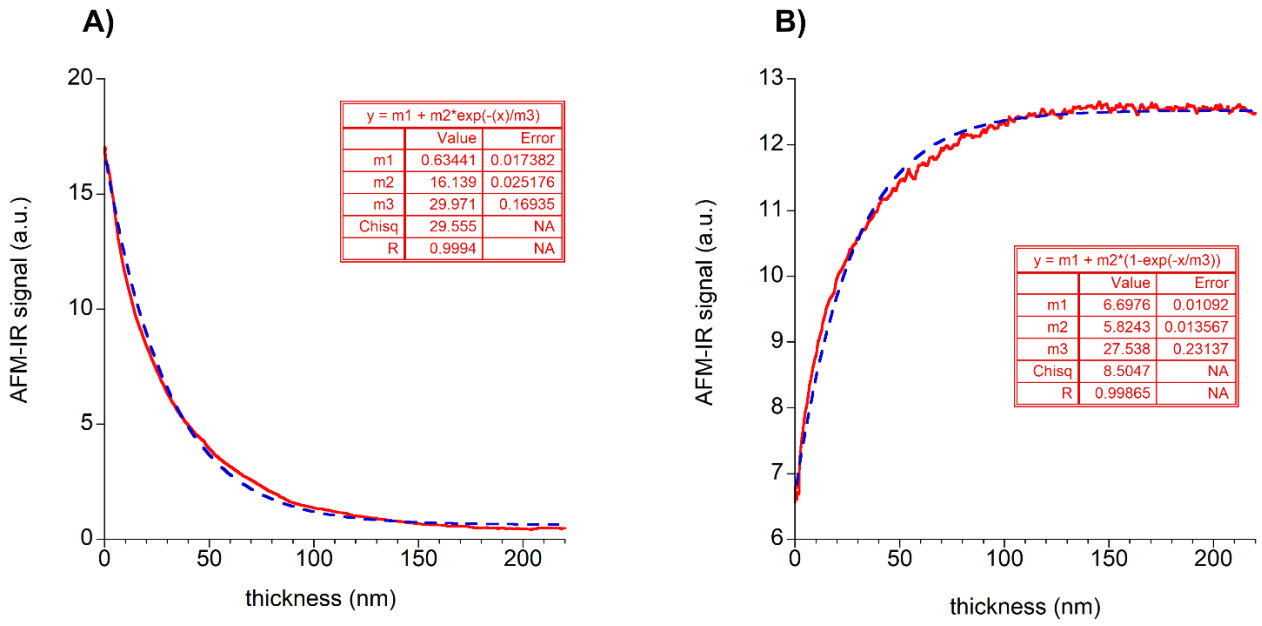

Fig. S4 : Calibration of probing depth for Tapping AFM-IR on the PS wedge on PMMA substrate using a gold coated 300kHz cantilever from Nanosensors. A) The red curve corresponds to the tapping AFM-IR signal as a function of the wedge thickness when the wavenumber is fixed at 1730 cm-1 (PMMA absorption only). In dashed blue the corresponding fit is given of the exponential decay used to estimate the probing depth (m3). B) The red curve corresponds to the tapping AFM-IR signal as a function of the wedge thickness when the wavenumber is fixed at 1600 cm-1 (PS absorption only). In dashed blue the corresponding fit is given of the exponential growth used to estimate the probing depth (m3).

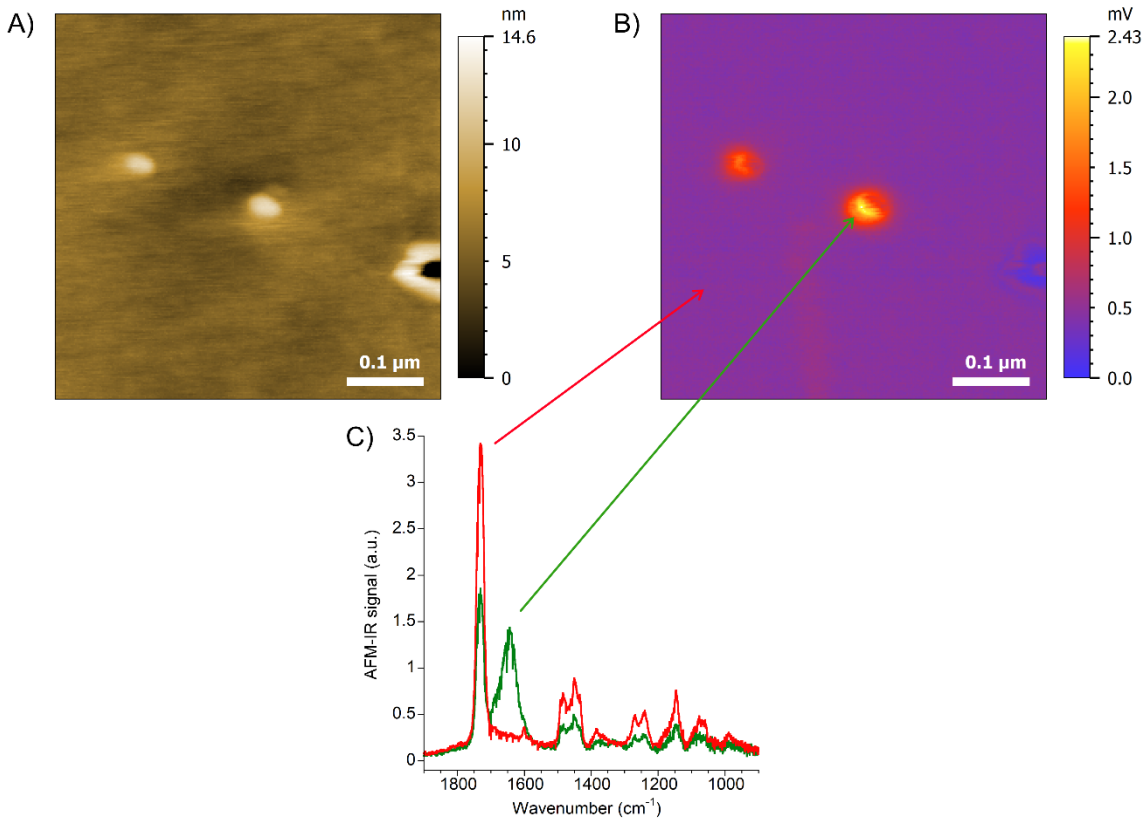

Fig. S5 : AFM-IR characterization of the nanoparticles on the PS-PMMA blend. A) Topography image showing the shape of typical nanoparticles. The diameter of these nanoparticles is around 60 nm at a height of 10 nm. B) Chemical map at 1625 cm^{-1} revealing the absorption of the nanoparticles. The matrix of PMMA has a smaller level of absorption at this wavenumber than the nanoparticles. C) Spectra realized on the corresponding map B. In red the spectrum corresponding to the PMMA matrix is given. In green we show the spectrum obtained on the nanoparticles. This spectrum shows bands belonging to PMMA, corresponding to the response of the surrounding matrix, and a specific band centered at 1625 cm^{-1} characteristic to a carbonyl group vibration.

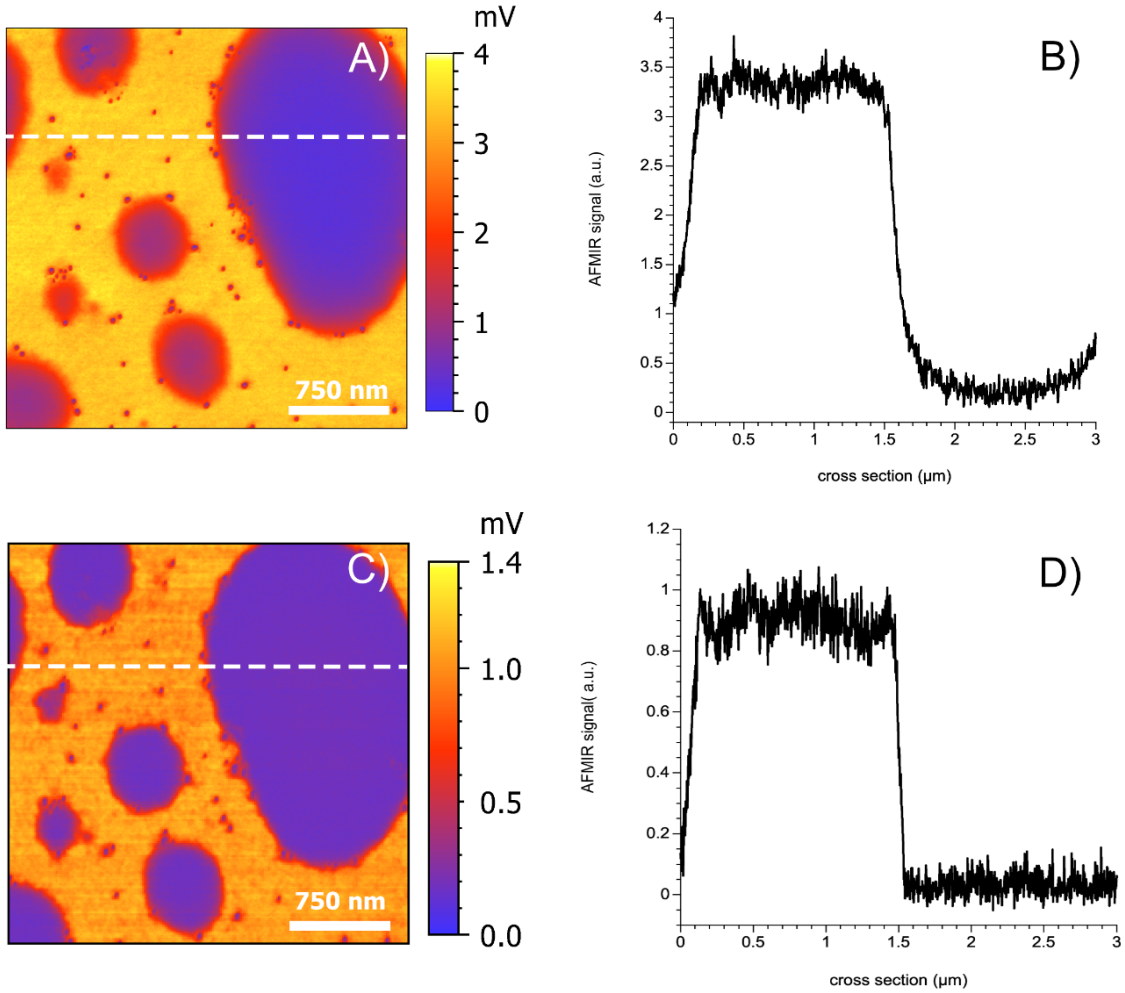

Fig. S6 : Comparison of chemical maps of the PS-PMMA blend for resonance enhanced and surface sensitive AFM-IR. A) IR map in resonance enhanced mode at 1730 cm^{-1} for a laser repetition rate f_{laser} = 2915kHz (corresponding to a probing depth of 40 nm). B) Cross section corresponding to the white dashed line in panel A showing the shape of the big PS domain at the right side of the image. The cross section clearly reveals the curvature of the domain and the fact that this mode has a probing depth long enough to feel the PMMA under the PS domain as the signal of absorption is not zero but 0.3 mV. C) IR map in surface sensitive mode (f_{laser}=2085kHz corresponding to 10 nm of probing depth). D) Cross section corresponding to the white dashed line in panel C showing the shape of the big PS domain at the right side of the image. The cross section in that case indicates that the absorption signal quickly goes to zero value when the tip is on the PS domain. This is due to the very short probing depth of the surface sensitive mode compared to the contact mode at 2915 kHz, meaning that the surface sensitive mode cannot probe beyond the thickness of this PS domain. Moreover, as the signal disappears on the PS sample, it confirms that there is no PMMA layer on the PS domain.

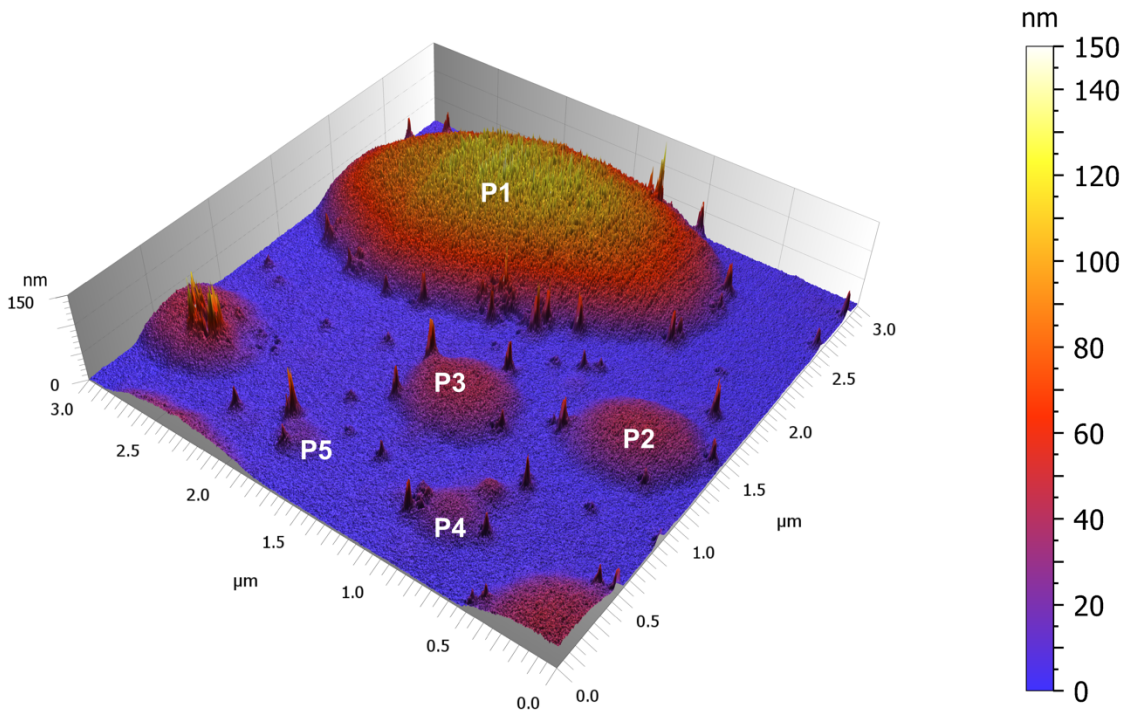

Fig. S7 : 3D tomography reconstruction of PS domains inside the PMMA matrix of the PS-PMMA blend using PS absorption maps.

The 3D tomography image has been constructed by averaging the AFM-IR absorption images obtained at 1600cm^{-1} (PS absorbs) for the 5 highest modes of the cantilever and the parameter I_0 has been adjusted to converge to the 138 nm thickness for the P1 sample. The 138 nm thickness target resulted from the tomography reconstruction based on the 1730cm^{-1} (PMMA absorption) absorption maps (see main text).